UC Berkeley

UC Berkeley Previously Published Works

Title

A simple way to test for collinearity in spin symmetry broken wave functions: General theory and application to generalized Hartree Fock

Permalink

https://escholarship.org/uc/item/9k031569

Journal

The Journal of Chemical Physics, 142(9)

ISSN

0021-9606

Authors

Small, David W
Sundstrom, Eric J
Head-Gordon, Martin

Publication Date

2015-03-07

DOI

10.1063/1.4913740

Peer reviewed

eScholarship.org Powered by the California Digital Library
University of California

A simple way to test for collinearity in spin symmetry broken wave functions: general theory and application to Generalized Hartree Fock

David W. Small and Eric J. Sundstrom and Martin Head-Gordon

Department of Chemistry, University of California,

Berkeley, California 94720 and Chemical Sciences Division,

Lawrence Berkeley National Laboratory, Berkeley, California 94720

(Dated: February 17, 2015)

Abstract

We introduce a necessary and sufficient condition for an arbitrary wavefunction to be collinear, i.e. its spin is quantized along some axis. It may be used to obtain a cheap and simple computational procedure to test for collinearity in electronic structure theory calculations. We adapt the procedure for Generalized Hartree Fock (GHF), and use it to study two dissociation pathways in CO_2. For these dissociation processes, the GHF wave functions transform from low-spin Unrestricted Hartree Fock (UHF) type states to noncollinear GHF states and on to high-spin UHF type states, phenomena that are succinctly illustrated by the constituents of the collinearity test. This complements earlier GHF work on this molecule.

I. INTRODUCTION

Electronic structure practitioners have long relied on spin-unrestricted Hartree Fock (UHF) and Density Functional Theory (DFT) for open-shell and strongly correlated systems. A key reason for this is that the latter's multiradical nature is partially accommodated by unrestricted methods: the paired spin-up and spin-down electrons are allowed to separate, while maintaining their spin alignment along a three-dimensional axis, i.e. their spin collinearity. But, considering the great potential for diversity in multitradical systems, it is not a stretch to concede that this approach is not always reasonable. For some of the more overt substantiations of this, we might look to spin frustrated systems, which, virtually by definition, defy the (single determinantal) idea of spin alignment. This category connects to important molecular examples, such as models of the core of the Photosynthetic Oxygen-Evolving Complex,[1–4] and also extended-system phenomena like noncollinear magnetism.[5–8] There are also more subtle reproaches to unchecked UHF usage. For example, tenable theoretical treatments of paramagnetic systems, such as liquid oxygen,[9] require a full range of spin orientations for their radical units. If one chooses to take the spin polarized, single-determinant approach for systems like any of these, the collinearity constraint of UHF should be removed, i.e. Generalized Hartree Fock (GHF) should be used.

GHF has been researched for a long time,[10–24] and while it has only rarely been used, it is gaining momentum. For example, GHF has recently been used to obtain interesting new perspectives on a variety of fullerenes.[25] The existing or potential application of noncollinearity in Electronic Structure Theory extends well beyond GHF, and we will mention a few examples now. GHF's DFT cousin, usually referred to as "noncollinear DFT", has received significant attention. The construction of noncollinear functionals is not as straightforward as in the collinear case, and so several schemes for this have been put forth and it remains an active research area.[26–37]

Noncollinearity is also of interest for correlated wavefunction-based approaches. Noncollinear wave functions are used to parameterize collinear, symmetry purified states in Projected Quasiparticle Theory.[38,39] Noncollinearity seems especially germane to geminal theory. UHF-type spin polarization has been incorporated into Generalized Valence Bond Perfect Pairing[40,41] and into other strongly orthogonal geminal approximations,[42–44] and including GHF-style polarization may be a sensible next step. We expect spin polarization

and noncollinearity to also be relevant for nonorthogonal geminal methods, such as recently developed ones based on the seniority concept.[45–51] We also note that there may be molecular systems for which the variationally optimal wave function in the Jastrow Antisymmetric Geminal Power approximation[52–57] is noncollinear.

Just as a UHF calculation may or may not actually break spin symmetry, a calculation in which noncollinearity is allowed may or may not produce a truely noncollinear result. Drawing a conclusion as to the latter is less trivial than it may seem. In GHF, for example, even if the canonical HF orbitals are a mixture of spin-up and spin-down parts, it does not imply noncollinearity, so a conclusion (usually) cannot be obtained by a casual inspection of orbital coefficients. Spin-symmetry breaking is usually quantified by the squared-total-spin expectation value, and an analogue of this for collinearity should be part of any noncollinear calculation. At this point, it is fitting to note that there exists a well-respected and rigorous classification of the various forms of HF, including UHF and GHF, which exhibits, among many things, certain distinguishing properties of noncollinear HF wave functions.[11] However, at least in our perception, the classification does not entail a practical procedure for collinearity testing, and even if we are incorrect on this matter, such methodology would be limited in the sense that it would be specific to HF wavefunctions. Thus, to our knowledge, this problem has not been adequately addressed before, and it is thereby the focus of this paper. We will develop some basic theory for general wave functions, specialize it to GHF, and apply the result to some simple GHF calculations.

II. THEORY

A. Collinearity for general wavefunctions

We will work with an arbitrary normalized wavefunction $|\Psi\rangle$ for n_o electrons. For the following, we define $\langle \mathbf{O} \rangle = \langle \Psi | \mathbf{O} | \Psi \rangle$, where $\mathbf{O}$ is any operator.

To determine if $|\Psi\rangle$ is collinear, we ask if it is an eigenvector of some axial spin operator, i.e. a spin operator associated with some Cartesian axis. More explicitly, we determine if there exists a unit vector $\mathbf{c} \in \mathbb{R}^3$ such that $|\Psi\rangle$ is an eigenvector of

$$\mathbf{c} \cdot \mathbf{S} = c_1 \mathbf{S}_1 + c_2 \mathbf{S}_2 + c_3 \mathbf{S}_3, \tag{1}$$

where $\mathbf{S} = (\mathbf{S}_x, \mathbf{S}_y, \mathbf{S}_z)^t$, the elements of this vector being the usual many-electron axial spin

operators.

It is useful to think of the varying candidate axes of our search as arising from rotations of the chosen z axis. Any such rotation is given by a 3x3 orthogonal matrix with determinant equal to 1, R, which rotates any point $\mathbf{c}$ to $R\mathbf{c}$. Likewise, $\mathbf{c}\cdot\mathbf{S}$ gets rotated to $(R\mathbf{c})\cdot\mathbf{S}$.

R will transform the x, y, z axes into a new set of axes; the columns of R are unit vectors corresponding to these axes. The familiar single-spin commutation relationships of the axial spin operators are valid for any set of spin axes forming a right-handed coordinate system, and these relationships, unlike the anticommutation ones, extend to the many-electron case:

$$[(R\mathbf{e}_j)\cdot\mathbf{S}, (R\mathbf{e}_k)\cdot\mathbf{S}] = \epsilon_{jkl}\, i\, (R\mathbf{e}_l)\cdot\mathbf{S}, \tag{2}$$

where $i = \sqrt{-1}$, $\mathbf{e}_j$ is the j-th column of the 3x3 identity matrix, I, and ϵ_{jkl} is the Levi-Civita symbol. For any set of axes, we can look at expectation values of the three associated spin operators

$$\chi_R = \Big(\langle (R\mathbf{e}_1)\cdot\mathbf{S}\rangle,\ \langle (R\mathbf{e}_2)\cdot\mathbf{S}\rangle,\ \langle (R\mathbf{e}_3)\cdot\mathbf{S}\rangle\Big)^t. \tag{3}$$

For every $\mathbf{y}\in\mathbb{R}^3$,

$$\langle \mathbf{y}\cdot\mathbf{S}\rangle = \mathbf{y}\cdot\Big(\langle \mathbf{S}_x\rangle,\ \langle \mathbf{S}_y\rangle,\ \langle \mathbf{S}_z\rangle\Big)^t = \mathbf{y}\cdot\chi_I, \tag{4}$$

so

$$\begin{aligned}\chi_R &= \Big((R\mathbf{e}_1)\cdot\chi_I,\ (R\mathbf{e}_2)\cdot\chi_I,\ (R\mathbf{e}_3)\cdot\chi_I\Big)^t \\ &= R^t\ \chi_I.\end{aligned} \tag{5}$$

Let $\epsilon_0 = \|\chi_I\|$, where we are using the Euclidean norm. We observe that $\|\chi_R\| = \epsilon_0$ for all rotation matrices R. In other words, ϵ_0 is a conserved quantity, and will thereby be useful.

Suppose temporarily that $|\Psi\rangle$'s spin is quantized in the direction corresponding to a unit vector $\mathbf{v}_0$. Without loss of generality, we may assume that the associated eigenvalue s is non-negative. There exists a rotation matrix R such that $R\mathbf{e}_3 = \mathbf{v}_0$. Then $(R\mathbf{e}_3)\cdot\mathbf{S}|\Psi\rangle = s|\Psi\rangle$. This, along with eq. (2), implies that the expectation values along the $R\mathbf{e}_1$ and $R\mathbf{e}_2$ axes must be zero. This means that $\chi_R = (0,0,s)^t = s\mathbf{e}_3$, which implies $s = \epsilon_0$. We next note that $\chi_I = R\chi_R = sR\mathbf{e}_3 = s\mathbf{v}_0$. Therefore, if $s \neq 0$, the quantization axis is given by $\mathbf{v}_0 = \epsilon_0^{-1}\chi_I$.

We return to the general case and consider the implications of the preceding paragraph. Of course, the eigenvalue spectrum of any axial spin operator is $\{-n_o/2, -n_o/2 +$

$1, \ldots, n_o/2 - 1, n_o/2\}$. If ϵ_0 is not one of these values, we definitely do not have a collinear state. For GHF wavefunctions, this property has been noted before.[17] If ϵ_0 is equal to one of the non-zero eigenvalues, then the quantization axis, if it exists, is in the direction given by $\mathbf{v}_0$. We may then simply test if $|\Psi\rangle$ is an eigenvector of $\mathbf{v}_0 \cdot \mathbf{S}$. A straightforward way to do this is to use

$$\mu(\mathbf{c}) = \langle (\mathbf{c} \cdot \mathbf{S})^2 \rangle - \langle \mathbf{c} \cdot \mathbf{S} \rangle^2. \tag{6}$$

This quantity is non-negative and is 0 if and only if $|\Psi\rangle$ is an eigenvector of $\mathbf{c} \cdot \mathbf{S}$. Therefore, in this case, we can simply evaluate $\mu(\mathbf{v}_0)$.

If $\epsilon_0 = 0$ and n_o is even, we do not immediately have a candidate direction for the potential quantization axis. But, we can develop a procedure that can be uniformly applied for any ϵ_0 value. Given the previously stated property of μ, we simply need to determine if this function has a root, i.e. a unit vector $\mathbf{c}$ such that $\mu(\mathbf{c}) = 0$. For this, we must first convert the expression for μ into one that is more readily usable.

For the first term on the RHS of eq. (6), it is straightforward to see that

$$\langle (\mathbf{c} \cdot \mathbf{S})^2 \rangle = \mathbf{c}^t X \mathbf{c}, \tag{7}$$

where

$$X = \begin{pmatrix} \langle \mathbf{S}_x^2 \rangle & \langle \mathbf{S}_x \mathbf{S}_y \rangle & \langle \mathbf{S}_x \mathbf{S}_z \rangle \\ \langle \mathbf{S}_y \mathbf{S}_x \rangle & \langle \mathbf{S}_y^2 \rangle & \langle \mathbf{S}_y \mathbf{S}_z \rangle \\ \langle \mathbf{S}_z \mathbf{S}_x \rangle & \langle \mathbf{S}_z \mathbf{S}_y \rangle & \langle \mathbf{S}_z^2 \rangle \end{pmatrix}. \tag{8}$$

X is Hermitian, and may well have complex off-diagonal elements, but because $\mathbf{c}$ is real, we only need the real part of X here.

For the second term on the RHS of eq. (6), we note that because the spin operators are Hermitian, χ_I is real. Combining this with eq. (4), we have

$$\langle \mathbf{c} \cdot \mathbf{S} \rangle^2 = (\mathbf{c} \cdot \chi_I)^2 = (\mathbf{c}^t \chi_I)(\chi_I^t \mathbf{c}) = \mathbf{c}^t (\chi_I \chi_I^t) \mathbf{c}. \tag{9}$$

Putting these results together, we have

$$\mu(\mathbf{c}) = \mathbf{c}^t A \mathbf{c}, \tag{10}$$

where

$$A = \mathrm{Re}(X) - \chi_I \chi_I^t. \tag{11}$$

A is Hermitian, indeed real symmetric, and $\mathbf{c}$ is normalized, so we can use the variational principle to see that the global minimum of μ is the lowest eigenvalue of A, which we will denote by μ_0. This establishes our collinearity test: $|\Psi\rangle$ is collinear if and only if $\mu_0 = 0$. If the latter is true, the axis of spin quantization is given by the eigenvector associated with μ_0.

To obtain computation-ready expressions for the constituents of the collinearity test, we find it convenient to work in second quantization, where we have

$$\mathbf{S}_m = \sum_{pq} (S_m)_{pq} \mathbf{a}_p^\dagger \mathbf{a}_q, \tag{12}$$

where m is x, y, or z, the p and q indices correspond to a set $\{\phi_p\}$ of orthonormal orbitals that spans the one-electron space, and

$$(S_m)_{pq} = \langle \phi_p | \mathbf{S}_m | \phi_q \rangle. \tag{13}$$

Using this, we get

$$\begin{aligned}
\mathbf{S}_m \mathbf{S}_n &= \sum_{pqrs} (S_m)_{pq} (S_n)_{rs} \mathbf{a}_p^\dagger \mathbf{a}_q \mathbf{a}_r^\dagger \mathbf{a}_s \\
&= \sum_{pqrs} (S_m)_{pq} (S_n)_{rs} \mathbf{a}_p^\dagger (\delta_{qr} - \mathbf{a}_r^\dagger \mathbf{a}_q) \mathbf{a}_s \\
&= \sum_{ps} (S_m S_n)_{ps} \mathbf{a}_p^\dagger \mathbf{a}_s + \sum_{prqs} (S_m)_{pq} (S_n)_{rs} \mathbf{a}_p^\dagger \mathbf{a}_r^\dagger \mathbf{a}_s \mathbf{a}_q \qquad (14) \\
&= \sum_{ps} (S_m S_n)_{ps} \mathbf{a}_p^\dagger \mathbf{a}_s + \sum_{p<r,q<s} (\mathfrak{S}_{mn})_{prqs} \mathbf{a}_p^\dagger \mathbf{a}_r^\dagger \mathbf{a}_s \mathbf{a}_q, \qquad (15)
\end{aligned}$$

where

$$\begin{aligned}
(\mathfrak{S}_{mn})_{prqs} = (S_m)_{pq} (S_n)_{rs} &- (S_m)_{rq} (S_n)_{ps} \\
&- (S_m)_{ps} (S_n)_{rq} + (S_m)_{rs} (S_n)_{pq},
\end{aligned} \tag{16}$$

this being the fully (anti)symmetrized form of the pertinent matrix elements. We therefore also have

$$\mathbf{S}_m \mathbf{S}_n = \sum_{ps} (S_m S_n)_{ps} \mathbf{a}_p^\dagger \mathbf{a}_s + \frac{1}{4} \sum_{prqs} (\mathfrak{S}_{mn})_{prqs} \mathbf{a}_p^\dagger \mathbf{a}_r^\dagger \mathbf{a}_s \mathbf{a}_q. \tag{17}$$

We may use these results to obtain

$$\langle \mathbf{S}_m \rangle = \sum_{pq} (S_m)_{pq} P_{pq} \tag{18}$$

and

$$\langle \mathbf{S}_m \mathbf{S}_n \rangle = \sum_{ps} (S_m S_n)_{ps} P_{ps} + \frac{1}{4} \sum_{prqs} (\mathfrak{S}_{mn})_{prqs} D^{pr}_{qs}, \tag{19}$$

where P and D are the one and two particle reduced density matrices for $|\Psi\rangle$, respectively.

The one-electron part of the RHS of eq. (19) can be simplified. For the one-electron spin space, we have the known properties

$$\hat{\mathsf{s}}_m^2 = \frac{1}{4} \mathsf{I}, \tag{20}$$

where I is the identity operator, and

$$\hat{\mathsf{s}}_m \hat{\mathsf{s}}_n = \epsilon_{mno} \frac{i}{2} \hat{\mathsf{s}}_o, \tag{21}$$

where m, n, o is any permutation of x, y, z, and ϵ_{mno} is the Levi-Civita symbol for the ordering x, y, z. These properties remain correct when we move to the one-electron spin-orbital space. This is because, in this space, the basic spin operators are given by a tensor product:

$$\hat{S}_m = I \otimes \hat{\mathsf{s}}_m, \tag{22}$$

the identity operator here being that for the spatial one-electron space. Of course, the actions of $\hat{S}_m$ and $\mathbf{S}_m$ coincide in the one-electron space. We have $\hat{S}_m \hat{S}_n = I \otimes \hat{\mathsf{s}}_m \hat{\mathsf{s}}_n$, etc., and the applicability of the above-mentioned properties follows. Since $S_m S_n$ is the matrix representation of $\hat{S}_m \hat{S}_n$ for the chosen orbital basis, we see that

$$\sum_{ps} (S_m S_m)_{ps} P_{ps} = \frac{1}{4} n_o \tag{23}$$

and

$$\mathrm{Re} \left(\sum_{ps} (S_m S_n)_{ps} P_{ps} \right) = 0, \quad \text{for } m \neq n, \tag{24}$$

so the term in parentheses in the latter equation does not contribute to the corresponding element of A. In the Appendix, we describe how A has a simplified block structure when $|\Psi\rangle$ happens to be a real wave function. We are now ready to apply the above results to GHF.

B. Specialization to GHF

We now assume that $|\Psi\rangle$ is a GHF or complex GHF (cGHF) wave function, and that $\{\phi_p\}$ is the molecular-orbital basis. Obtaining computable forms for the necessary spin

expectation values is much like deriving the usual expression for the HF energy; eqs. (12) and (15) bear a clear resemblance to the second-quantization form of the Hamiltonian operator. First, we have

$$\langle \mathbf{S}_m \rangle = \sum_{i=1}^{n_o} (S_m)_{ii} = \mathrm{tr}(O_m), \tag{25}$$

where the latter is the trace of O_m, the occupied-occupied block of S_m. Next, applying eq. (15) and grouping equal terms, we obtain

$$\begin{aligned} \langle \mathbf{S}_m \mathbf{S}_n \rangle &= \sum_{i=1}^{n_o} (S_m S_n)_{ii} + \sum_{i,j=1}^{n_o} \Big((S_m)_{ii}(S_n)_{jj} - (S_m)_{ij}(S_n)_{ji} \Big) \\ &= \sum_{i=1}^{n_o} (S_m S_n)_{ii} + \langle \mathbf{S}_m \rangle \langle \mathbf{S}_n \rangle - \mathrm{tr}(O_m O_n). \end{aligned} \tag{26}$$

When we substitute this into eq. (11), the $\langle \mathbf{S}_m \rangle \langle \mathbf{S}_n \rangle$ term will be cancelled by the corresponding element of $\chi_I \chi_I^t$. Incorporating eqs. (23) and (24), and noting that the trace of a product of Hermitian matrices is real, we obtain

$$A_{mn} = -\mathrm{tr}(O_m O_n) + \delta_{mn} \frac{1}{4} n_o. \tag{27}$$

These elements may be readily computed via

$$O_m = C^* \left(L \otimes \frac{1}{2} \sigma_m \right) C, \tag{28}$$

where C is the matrix of occupied orbital coefficients, * denotes the conjugate transpose, L is the overlap matrix for the spatial atomic orbital basis, and σ_x, σ_y, and σ_z are the Pauli matrices. Note that this equation corresponds to lexicographically ordered atomic spin orbitals in which the spatial component lies to the left of the spin part, i.e. the sequence is $\psi_1\alpha$, $\psi_1\beta$, $\psi_2\alpha$, $\psi_2\beta$, ….

III. GHF CALCULATIONS

We used the cc-pVDZ[58] basis and the Q-Chem program[59] for all calculations in this section.

In what follows, "GHF" will generally be used to refer to explicitly real GHF code and things that have been computed with it, regardless of the collinearity statuses of the results. In the same way, "cGHF" will be used to refer to calculations employing complex expansion

coefficients, without necessarily implying conclusions as to the collinearity or fundamental complexity of the results.

In all of the following examples, we performed HF stability analyses.[60] In the GHF case, we checked for internal instabilities, in which the energy may be lowered by orbital rotations within the domain of GHF, and external instabilities, where the energy may be lowered by rotations into the cGHF domain. The results of the former analysis will be stated as "GHF $\rightarrow$ GHF stable" or "GHF $\rightarrow$ GHF unstable", and we will use "GHF $\rightarrow$ cGHF ..." for the latter analysis. Again, these stability statuses pertain to the type of code being used, and are not being used to imply anything about collinearity nor fundamental complexity.

A. CO_2: Symmetric Dissociation

For this example, we consider linear $D_{\infty h}$ geometries of CO_2 of varying C-O bond lengths. For this PES, UHF cannot qualitatively describe the ground state at dissociation. In this region, the ground state is a coupling of the three triplet atoms into an overall singlet. UHF treats the unpaired electrons of triplet entities with an $\alpha\alpha$ or a $\beta\beta$ in the spin component. Defining m_s to be the spin quantum number along the principle axis, three copies of the preceding two spin vectors cannot be combined into an overall $m_s = 0$ state, which is how UHF approximates singlets. Under $m_s = 0$ constraints, the best UHF can do is put an $\alpha\alpha$ on one atom, an $\beta\beta$ on another atom, and an $\alpha\beta$ on the third atom. For the third atom, these two spins are attached to different p orbitals, which corresponds to an equal-weighted combination of the atom's triplet ground state and its open-shell singlet counterpart, which is higher in energy. The $m_s = 0$ UHF energy at dissociation is therefore higher than the sum of the ground-state energies of the three atoms.

In the dissociation limit, the singlet ground state becomes degenerate with some higher-multiplicity ground states, some of which can be qualitatively approximated with UHF. The overall lowest-energy UHF solution puts an $\alpha\alpha$ on two of the atoms and a $\beta\beta$ on the third atom, giving a $m_s = 1$ state with no singlet component. Unlike the $m_s = 0$ case, the $m_s = 1$ energy is size consistent. This is also true in the $m_s = 3$ case, where, at dissociation, an $\alpha\alpha$ is assigned to each atom.

It is of interest to see if GHF can improve on the preceding UHF problems. Such GHF explorations have appeared in a recent paper,[23] which we will refer to as "JHS11". In JHS11

Fig. 6, the authors show a zoom-in on the PES region in which spin-symmetry breaking HF solutions break away from RHF. Two of the shown curves are labelled as GHF and, within a certain bond-length range, are lower in energy than the shown UHF curves. We observe that one of the "GHF" solutions appears to coalesce with a UHF solution, which is also asserted by the JHS11 authors, yet the curve is still labelled "GHF" in that region. Accordingly, we do not assume that the JHS11 authors are strictly claiming these two curves correspond to noncollinear solutions, but rather that they are merely indicating that the curves are the lowest-energy results found with their GHF code. Thus these two HF solutions are appropriate for application of our collinearity test. We would like to make it clear that the purpose here is to further clarify the corresponding results of JHS11, not dispute them.

Using our GHF code, we isolated two HF solutions, hereafter denoted as sol. 1 and sol. 2, that, at least in terms of energy, match those found in JHS11 as discussed above. We plot the corresponding curves in Fig. 1. Firstly, we need to make a note regarding the comparison of this figure and JHS11 Fig. 6. We did stability analyses for the sol. 2 data, which showed GHF $\rightarrow$ GHF (and GHF $\rightarrow$ cGHF) stability from bond lengths 1.63 Å up to at least 1.8 Å, the latter being the rightmost point we considered for this solution. Sol. 2 is GHF $\rightarrow$ GHF unstable to the left of 1.63 Å, which may be a reason that, in JHS11 Fig. 6, the sol. 2 curve does not continue to the left of about 1.6 Å. We found that by using Direct Inversion of the Iterative Subspace (DIIS),[61,62] sol. 2 could be followed to the left indefinitely. Moving on, Fig. 1 also includes the basic results of the collinearity test. Indeed, each solution is truely noncollinear for some geometries. However, each solution is actually collinear for more than half of the shown bond-length range.

The details of the collinearity test for sol. 2 are shown in Fig. 2, where we plot ϵ_0 and μ_0. To the left of 1.6 Å, μ_0 and ϵ_0 are both 0, which indicates that in this region the solution is equivalent to an $m_s = 0$ UHF solution, in fact one that does not appear in JHS11 Fig. 6. To the right of 1.7 Å, μ_0 returns to a value of 0, while here ϵ_0 settles to a value of 1. This confirms that this GHF solution coalesces with a $m_s = 1$ UHF solution, as stated in JHS11. To summarize these results, sol. 2 may be characterized as an $m_s = 0$ UHF solution that undergoes a local (in the sense that only some of the spins are rotated) noncollinear spin rotation to end up as an $m_s = 1$ UHF solution. Interestingly, moving to the left, it appears that sol. 2 is not heading toward coalescence with the RHF curve. Indeed, this solution remains spin-symmetry broken at least down to 1 Å. It reaches a minimum at around 1.27

Å, where it has $\langle \mathbf{S}^2 \rangle = 1.34$ and a binding energy of 82.8 kcal/mol. In this case, GHF is not producing the "desired" result of connecting the lowest-energy UHF at equilibrium, i.e. RHF, to the lowest-energy UHF at dissociation.

Moving to the right in JHS11 Fig. 6, sol. 1 does not appear to be joining with any shown UHF solution. To investigate this, we attempted to track our sol. 1 into the dissociation region. We ran stability analyses, which showed that sol. 1 is GHF $\rightarrow$ GHF (and GHF $\rightarrow$ cGHF) stable from 1.46 to 1.79 Å, after which it becomes GHF $\rightarrow$ GHF unstable. For longer bond lengths, we found that it is possible to remain on sol. 1 indefinitely by using DIIS. The principal components of the collinearity test are shown in Fig. 3. From the μ_0 curve, we see that sol. 1 is noncollinear for a wide range of geometries, but eventually returns to collinearity to the right of about 2.5 Å. In the noncollinear region, μ_0 exhibits singularities at around 1.8 and 2.4 Å. These are the result of crossings, or possibly very narrow avoided crossings, in the eigenvalues of the A matrix. Accordingly, in Fig. 3 we have included curves for the other two eigenvalues, which we label μ_1 and μ_2. Note the μ_1-μ_2 degeneracy at collinear geometries, which is one manifestation of the familiar fact that any two orthogonal axes spanning the plane perpendicular to the primary spin axis of a (non-RHF) UHF solution are equivalent to each other.

We plot the sol. 1 energy in Fig. 4. The curve goes over a hump and eventually dissociates to the ground-state limit described above. Sol. 1's nature can be understood by looking at its ϵ_0 curve, which is shown in Fig. 4. We first observe that over most of the range shown, the ϵ_0 value is not an integer, which indicates noncollinearity. In this case, μ_0 is needed only when ϵ_0 is 0, 1, 2, or 3. Given the μ_0 results, the ϵ_0 curve shows that sol. 1 may be characterized as an $m_s = 0$ UHF solution that undergoes a local noncollinear spin rotation to end up as an $m_s = 3$ UHF solution. This rotation is quite a bit more significant than that observed in sol. 2, because sol. 1 transforms from a singlet-type wave function to a septet-type wave function, entailing complete rotations of three spins. Sol. 1 also does not appear to be heading toward coalescence with the RHF curve; indeed, JHS11 Fig. 6 shows that sol. 1 and RHF cross. The JHS11 authors were unable to track sol. 1 to the left of 1.46 Å, and neither were we: we separately tried the Maximum Overlap Method,[63] SCF Metadynamics,[64] and cGHF, including combining these with various optimization algorithms, but to no avail. We do note that, moving to the left, sol. 1's $\langle \mathbf{S}^2 \rangle$ value is rapidly decreasing: it is 1.35, 1.25, 1.14, and 0.93 at 1.49, 1.48, 1.47, and 1.46 Å, respectively. Thus sol. 1 may be heading

towards coalescence with an RHF solution.

In Figs. 2 and 4, we have included data for $\langle \mathbf{S}_x \rangle$ and $\langle \mathbf{S}_z \rangle$ to illustrate that although collinear, i.e. essentially UHF, solutions may be found with GHF code, they will generally be spin rotations of, and thereby not *exactly* the same as, their counterparts computed with traditional UHF codes. For example, both solutions exhibit non-zero values for $\langle \mathbf{S}_x \rangle$ even when they are collinear, which cannot occur in a traditional UHF computation.

B. CO_2: Asymmetric Dissociation

Another interesting aspect of CO_2 is its asymmetric dissociation into CO and O, which is also found in JHS11. Following those authors, we will consider linear geometries with one C-O bond fixed at 1.16 Å, while varying the other C-O bond length. Since the ground state of CO_2 at equilibrium is singlet, and the ground states of CO and O are singlet and triplet, respectively, the asymmetric dissociation involves a true intersystem crossing.

In JHS11 Fig. 9, there are two curves labelled as GHF. We have reproduced, again in terms of matching energies, these two solutions with our GHF code, and we plot them, along with the basic results of collinearity testing, in Fig. 5. For this, we first found sol. 1, starting at 1.7 Å. We followed the solution down to 1.63 Å, whereupon it becomes RHF. Also starting from the initial 1.7 Å point, we followed sol. 1 to the right. At 1.78 Å, sol. 1 becomes GHF → cGHF unstable, but it remains GHF → GHF stable up until 1.81 Å, after which it becomes unstable. Using DIIS, we were able to follow sol. 1 to the right indefinitely. To recap, sol. 1 is GHF → cGHF stable from 1.63 Å up until 1.77 Å and GHF → GHF stable from 1.63 Å up until 1.81 Å. We plot the energy and μ_0 curves for sol. 1 in Fig. 6. For sol. 1, $\epsilon_0 = 0$ at all points shown. This gives us no information regarding collinearity, so this is a good example of when we must rely on μ_0. Sol. 1 is noncollinear for all points to the right of 1.63 Å. It is of note that its relative energy does not approach 0 in the dissociation limit. In fact, its energy limit is lower than the sum of the $m_s = 0$ CO and $m_s = 0$ O UHF energies. We were unable to find any HF solutions for CO and O that match the dissociation limit of sol. 1. It is possible that no such solutions exist, akin to how the RHF energy in the dissociation of a covalent bond does not correspond to any HF energies for the associated atoms. An analysis of local spin populations may be helpful here, but this is getting outside the present scope, and we have not yet implemented such capabilities in our GHF code.

We obtained sol. 2 by following the GHF → cGHF instability of sol. 1 at 1.78 Å, and then following this to the left and right. All of our data for sol. 2 was obtained with our cGHF code. Given that this data energetically matched the JHS11 curve, which was obtained with explicitly real orbitals, we suspected that our sol. 2 is equivalent to a real GHF solution. Indeed, for one geometry, we used our GHF code to try to obtain a solution of the same energy as that from our cGHF code, and were successful. It is therefore likely that our cGHF-code sol. 2 is equivalent to the solution found in JHS11. However, it must be noted that this is not a proof that our sol. 2 is fundamentally real, this requiring a different testing procedure.

We plot the ϵ_0 and μ_0 curves for sol. 2 in Fig. 7. As was the case for symmetric-dissociation sol. 1, sol. 2 here exhibits a crossing in the μ_0 curve. Fig. 7 reveals that sol. 2 is a local noncollinear spin rotation of an $m_s = 0$ UHF solution into an $m_s = 1$ UHF solution. The JHS11 authors state that sol. 2 connects to the $m_s = 1$ UHF curve, but do not assert that it connects to the $m_s = 0$ UHF curve; indeed, the JHS11 Fig. 9 curve appears to come to a halt to the left of 1.77 Å. This may relate to the observation that in moving from 1.77 to 1.76 Å, our sol. 2 goes from being cGHF → cGHF stable to unstable, i.e. the solution is unstable to the left of this point, and stable to the right. We note in passing that this means that sol. 1 and sol. 2 are both stable at e.g. 1.77 Å. We did many cGHF calculations (at intervals of 0.001 Å) in this region to confirm that sol. 2 indeed coalesces with the $m_s = 0$ UHF curve. Thus, in contrast to the symmetric-dissociation case, here GHF is able to connect the lowest equilibrium solution to the lowest solution at dissociation. It should be noted that these UHF solutions are approximating exact states of differing spin multiplicities, so their connection is unphysical, considering the absence of spin-orbit coupling.

Finally, we have plotted $\langle \mathbf{S}_x \rangle$ and $\langle \mathbf{S}_z \rangle$ for sol. 2 in Fig. 8. We did not include $\langle \mathbf{S}_y \rangle$ because its curve looks just like that for ϵ_0. We note that non-zero values for $\langle \mathbf{S}_y \rangle$, such as those found here, would not be possible within an (explicitly real) GHF code, as shown in the Appendix. As stated previously, we think that sol. 2 is equivalent to a real GHF solution, which would have a $\langle \mathbf{S}_y \rangle$ value of 0. As do the above examples, this illustrates the point that HF solutions whose *exact* forms can be obtained only with a GHF or cGHF calculation are not necessarily noncollinear nor fundamentally complex; these "simpler" HF solutions can take on diverse appearances when they show up in GHF and cGHF calculations. In contrast, non-zero $\langle \mathbf{S}_y \rangle$ values can have more physically meaningful implications when they

arise in fundamentally complex GHF solutions, such as those reported recently for various fullerenes.[25]

IV. DISCUSSION AND CONCLUSIONS

In this paper, we have introduced a simple collinearity test that may be applied to any spin-symmetry broken wave function. To summarize the test, a wave function is collinear if and only if $\mu_0 = 0$, where

$$\mu_0 = \min_{\mathbf{c}\in\mathcal{S}^2} \left(\langle (\mathbf{c}\cdot\mathbf{S})^2 \rangle - \langle \mathbf{c}\cdot\mathbf{S} \rangle^2 \right), \tag{29}$$

with $\mathcal{S}^2$ being the unit sphere. μ_0 and the minimizing $\mathbf{c}$ are obtained by computing the lowest eigenpair of the matrix defined in eq. (11) (see also eq. (27) for the GHF case). Also useful is

$$\epsilon_0 = \sqrt{\langle \mathbf{S}_x \rangle^2 + \langle \mathbf{S}_y \rangle^2 + \langle \mathbf{S}_z \rangle^2}, \tag{30}$$

which indicates noncollinearity if it is not an allowed value of $|m_s|$, this fact having been utilized previously for the GHF case.[17] When ϵ_0 is an allowed value of $|m_s|$, no collinearity conclusion may be drawn without further information, and so μ_0 serves to complete the picture. In the GHF case, if $\mu_0 = 0$, the wave function is equivalent to a UHF wave function with $\frac{1}{2}(n_\alpha - n_\beta) = \epsilon_0$, and so plots of μ_0 and ϵ_0 effectively characterize GHF solutions.

We focused on the test's application to GHF and cGHF calculations. The test may be performed at the end of such calculations, with a cost negligible compared to that of the SCF optimization steps. We studied two dissociation pathways for CO_2. The components of the collinearity test provided a clear picture of the basic physical character of the pertinent HF solutions: they showed how $m_s = 0$ UHF solutions in the equilibrium region undergo noncollinear spin rotations in GHF to connect to the lowest-energy UHF solutions in the dissociation region, which have nonzero m_s values. To our knowledge, the observations that the pertinent GHF solutions connect to disparate UHF solutions in *both* of these regions are novel results for this molecule, thus complementing earlier work on it.

We showed that, in the CO_2 asymmetric dissociation, GHF is able to connect the lowest HF solutions at equilibrium and dissociation. However, the pertinent solution is not always the lowest-energy one. It is of interest to see if this remains true when larger basis sets and/or other methods, e.g. noncollinear DFT methods, are used. In contrast, GHF does not appear

to be able to make such connections in the symmetric dissociation. It is possible that this occurs in one of the solutions, but a conclusion on this matter was prevented by numerical difficulties. These GHF behaviors are in opposition with the exact ground-state PES's: the latter involves a crossing in the asymmetric dissociation, but not in the symmetric one. This is just one example of the generally known fact that GHF can sometimes connect states of different spin multiplicities, which is technically unphysical in the absence of e.g. spin-orbit interactions. We argue that more experimentation with GHF is needed to determine if this kind of behavior is ultimately useful or detrimental.

Our CO_2 asymmetric dissociation calculations touched on an interesting aspect of SCF optimizations. For sol. 1 at 1.78 Å, the energy is GHF $\rightarrow$ GHF stable and GHF $\rightarrow$ cGHF unstable. However, the lower-energy solution to which this instability leads is, we think, another (real) GHF solution. In other words, the tools associated with a more complicated HF level (in this case cGHF) were able, indeed required, to find the connection between two solutions of a simpler HF level (in this case real GHF). We have observed analogous behavior for other molecules and different HF levels, as have other researchers.[47] It would be of interest to further study this phenomenon. However, it should be recognized that it is not always operative: in the CO_2 asymmetric dissociation, sol. 2 is the upper curve at 1.77 Å, yet it is cGHF $\rightarrow$ cGHF stable there. This exemplifies the fact that stability analysis only tests whether a solution is a local minimum.

We close by stating that the collinearity test may be employed as part of a practical realization of Fukutome's classification of determinantal wave functions.[11] Using the terminology employed by Fukutome, the test distinguishes between spin axial and torsional HF wave functions. Essentially, the two remaining facets of the classification are concerned with time reversal symmetry and the "magnetic operations". It can be shown that the latter relate to the separation of essentially real wavefunctions and ones that are fundamentally complex. The goal of putting these concepts into practical computational usage and joining the result with the collinearity test lays ground for future work.

ACKNOWLEDGMENTS

Part of this work was supported by the Office of Science, Office of Basic Energy Sciences, of the (U.S.) Department of Energy under Contract No. DE-AC02-05CH11231. M.H.-G. is

a part-owner of Q-CHEM Inc.

APPENDIX: BLOCK STRUCTURE OF A FOR REAL $|\Psi\rangle$

Here, we will comment on the simplified structure of A when $|\Psi\rangle$ is a real wave function. As to the latter property, we mean that for any real one-electron basis, every coefficient of $|\Psi\rangle$'s expansion relative to the corresponding determinants is real. To be precise regarding the reality of the one-electron basis, the usual one-electron spin states, α and β, are taken to be real. For simplicity, we will here choose the ϕ_p to be of the form $\zeta_p\omega_j$, where the ζ_j form a set of real orthonormal spatial orbitals and ω_j is α or β. The corresponding one and two electron density matrices for $|\Psi\rangle$ are real. We have $\langle\zeta_p\omega_j|\mathbf{S}_m|\zeta_q\omega_k\rangle = \delta_{pq}(\sigma_m)_{jk}/2$, where σ_x, σ_y, and σ_z are the Pauli matrices. It follows that S_y is purely imaginary and S_x and S_z are purely real. This means that $\mathfrak{S}_{xy}$, $\mathfrak{S}_{yx}$, $\mathfrak{S}_{yz}$, and $\mathfrak{S}_{zy}$ are purely imaginary. As with the two-electron integral array, $\mathfrak{S}_{mn}$ is a Hermitian matrix, where we are grouping indices 1 and 2 into a compound index, and likewise with indices 3 and 4. In the same way, the two-electron density matrix is Hermitian. The trace of a product of two Hermitian matrices, one purely imaginary and the other purely real, is 0. Applying this to eqs. (18) and (19), we see that in the present case, $\langle\mathbf{S}_y\rangle$ is 0, as are the two-electron parts of $\langle\mathbf{S}_x\mathbf{S}_y\rangle$, $\langle\mathbf{S}_y\mathbf{S}_x\rangle$, $\langle\mathbf{S}_y\mathbf{S}_z\rangle$, and $\langle\mathbf{S}_z\mathbf{S}_y\rangle$. Therefore, in this case, $A_{xy} = A_{yx} = A_{yz} = A_{zy} = 0$, i.e. the matrix has a block structure. Both blocks need to be considered in the collinearity test.

[1] E. Libby, J. K. McCusker, E. A. Schmitt, K. Folting, D. N. Hendrickson, and G. Christou, Inorg. Chem. **30**, 3486 (1991).

[2] G. Charles Dismukes and R. T. van Willigen, *Manganese: The Oxygen-Evolving Complex & Models* (John Wiley & Sons, Ltd, 2006).

[3] E. M. Sproviero, J. A. Gascón, J. P. McEvoy, G. W. Brudvig, and V. S. Batista, Coord. Chem. Rev. **252**, 395 (2008).

[4] S. Luo, I. Rivalta, V. Batista, and D. G. Truhlar, J. Phys. Chem. Lett. **2**, 2629 (2011).

[5] D. Hobbs and J. Hafner, in *Annals of the Marie Curie Fellowship Association*, edited by V. Charmandaris, volume 4 of *Annals of the Marie Curie Fellowship Association*, pp. 1–6 (Marie Curie Fellowship Association, 2006).

[6] S. Lounis, J. Phys.: Condens. Matter **26**, 273201 (2014).

[7] L. M. Sandratskii, Adv. Phys. **47**, 91 (1998).

[8] J. M. D. Coey, Can. J. Phys. **65**, 1210 (1987).

[9] T. Oda and A. Pasquarello, Phys. Rev. B **70**, 134402 (2004).

[10] K. Yamaguchi, Chem. Phys. **25**, 215 (1977).

[11] H. Fukutome, Int. J. Quantum Chem. **20**, 955 (1981).

[12] B. Sykja and J.-L. Calais, J. Phys. C Solid State **15**, 3079 (1982).

[13] B. Sykja and J.-L. Calais, Theor. Chim. Acta **62**, 429 (1983).

[14] J.-L. Calais, Adv. Quantum Chem. **17**, 225 (1985).

[15] P.-O. Löwdin and I. Mayer, Adv. Quantum Chem. **24**, 79 (1992).

[16] I. Mayer and P.-O. Löwdin, Chem. Phys. Lett. **202**, 1 (1993).

[17] S. Hammes-Schiffer and H. C. Andersen, J. Chem. Phys. **99**, 1901 (1993).

[18] K. Yamaguchi, S. Yamanaka, M. Nishino, Y. Takano, Y. Kitagawa, H. Nagao, and Y. Yoshioka, Theor. Chem. Acc. **102**, 328 (1999).

[19] D. Yamaki, Y. Shigeta, S. Yamanaka, H. Nagao, and K. Yamaguchi, Int. J. Quantum Chem. **84**, 546 (2001).

[20] T. Kawakami, R. Takeda, S. Nishihara, T. Saito, M. Shoji, S. Yamada, S. Yamanaka, Y. Kitagawa, M. Okumura, and K. Yamaguchi, J. Phys. Chem. A **113**, 15281 (2009).

[21] J. Stuber and J. Paldus, in *Fundamental World of Quantum Chemistry. A Tribute to the Memory of Per-Olov Löwdin*, edited by E. J. Brändas and E. S. Kryachko, volume 1, pp. 67–139 (Kluwer Academic Publishers, Dordrecht, The Netherlands, 2003).

[22] F. Cavaliere and U. De Giovannini, Physica E **42**, 606 (2010).

[23] C. A. Jiménez-Hoyos, T. M. Henderson, and G. E. Scuseria, J. Chem. Theory Comput. **7**, 2667 (2011).

[24] Y. Cui, I. W. Bulik, C. A. Jiménez-Hoyos, T. M. Henderson, and G. E. Scuseria, J. Chem. Phys. **139**, 154107 (2013).

[25] C. A. Jiménez-Hoyos, R. Rodríguez-Guzmán, and G. E. Scuseria, J. Phys. Chem. A **118**, 9925 (2014).

[26] J. Kübler, K.-H. Höck, J. Sticht, and A. R. Williams, J. Phys. F: Met. Phys. **18**, 469 (1988).

[27] T. Oda, A. Pasquarello, and R. Car, Phys. Rev. Lett. **80**, 3622 (1998).

[28] D. Hobbs, G. Kresse, and J. Hafner, Phys. Rev. B **62**, 11556 (2000).

[29] S. Yamanaka, D. Yamaki, Y. Shigeta, H. Nagao, Y. Yoshioka, N. Suzuki, and K. Yamaguchi, Int. J. Quantum Chem. **80**, 664 (2000).

[30] K. Capelle and L. N. Oliveira, Phys. Rev. B **61**, 15228 (2000).

[31] H. Yamagami, Phys. Rev. B **61**, 6246 (2000).

[32] P. Kurz, F. Förster, L. Nordström, G. Bihlmayer, and S. Blügel, Phys. Rev. B **69**, 024415 (2004).

[33] J. E. Peralta, G. E. Scuseria, and M. J. Frisch, Phys. Rev. B **75**, 125119 (2007).

[34] S. Sharma, J. K. Dewhurst, C. Ambrosch-Draxl, S. Kurth, N. Helbig, S. Pittalis, S. Shallcross, L. Nordström, and E. K. U. Gross, Phys. Rev. Lett. **98**, 196405 (2007).

[35] F. G. Eich and E. K. U. Gross, Phys. Rev. Lett. **111**, 156401 (2013).

[36] G. Scalmani and M. J. Frisch, J. Chem. Theory Comput. **8**, 2193 (2012).

[37] I. W. Bulik, G. Scalmani, M. J. Frisch, and G. E. Scuseria, Phys. Rev. B **87**, 035117 (2013).

[38] G. E. Scuseria, C. a. Jiménez-Hoyos, T. M. Henderson, K. Samanta, and J. K. Ellis, J. Chem. Phys. **135**, 124108 (2011).

[39] C. a. Jiménez-Hoyos, T. M. Henderson, T. Tsuchimochi, and G. E. Scuseria, J. Chem. Phys. **136**, 164109 (2012).

[40] G. J. O. Beran, B. Austin, A. Sodt, and M. Head-Gordon, J. Phys. Chem. A. **109**, 9183 (2005).

[41] K. V. Lawler, D. W. Small, and M. Head-Gordon, J. Phys. Chem. A **114**, 2930 (2010).

[42] V. A. Rassolov, J. Chem. Phys. **117**, 5978 (2002).

[43] V. A. Rassolov and F. Xu, J. Chem. Phys. **126**, 234112 (2007).

[44] P. Jeszenszki, V. Rassolov, P. R. Surján, and A. Szabados, Mol. Phys. (2014), in press.

[45] P. A. Limacher, P. W. Ayers, P. A. Johnson, S. De Baerdemacker, D. Van Neck, and P. Bultinck, J. Chem. Theory Comput. **9**, 1394 (2013).

[46] P. A. Johnson, P. W. Ayers, P. A. Limacher, S. D. Baerdemacker, D. V. Neck, and P. Bultinck, Comp. Theor. Chem. **1003**, 101 (2013).

[47] P. A. Limacher, T. D. Kim, P. W. Ayers, P. A. Johnson, S. De Baerdemacker, D. Van Neck, and P. Bultinck, Mol. Phys. **112**, 853 (2014).

[48] K. Boguslawski, P. Tecmer, P. W. Ayers, P. Bultinck, S. De Baerdemacker, and D. Van Neck, Phys. Rev. B **89**, 201106 (2014).

[49] K. Boguslawski, P. Tecmer, P. A. Limacher, P. A. Johnson, P. W. Ayers, P. Bultinck, S. De Baerdemacker, and D. Van Neck, J. Chem. Phys. **140**, 214114 (2014).

[50] L. Bytautas, T. M. Henderson, C. A. Jiménez-Hoyos, J. K. Ellis, and G. E. Scuseria, J. Chem. Phys. **135**, 044119 (2011).

[51] T. Stein, T. M. Henderson, and G. E. Scuseria, J. Chem. Phys. **140**, 214113 (2014).

[52] M. Casula and S. Sorella, J. Chem. Phys. **119**, 6500 (2003).

[53] M. Casula, C. Attaccalite, and S. Sorella, J. Chem. Phys. **121**, 7110 (2004).

[54] A. Zen, E. Coccia, Y. Luo, S. Sorella, and L. Guidoni, J. Chem. Theory Comput. **10**, 1048 (2014).

[55] E. Neuscamman, Phys. Rev. Lett. **109**, 203001 (2012).

[56] E. Neuscamman, J. Chem. Phys. **139**, 181101 (2013).

[57] E. Neuscamman, J. Chem. Phys. **139**, 194105 (2013).

[58] T. H. Dunning, J. Chem. Phys. **90**, 1007 (1989).

[59] Y. Shao, Z. Gan, E. Epifanovsky, A. T. Gilbert, M. Wormit, J. Kussmann, A. W. Lange, A. Behn, J. Deng, X. Feng, D. Ghosh, M. Goldey, P. R. Horn, L. D. Jacobson, I. Kaliman, R. Z. Khaliullin, T. Kuś, A. Landau, J. Liu, E. I. Proynov, Y. M. Rhee, R. M. Richard, M. A. Rohrdanz, R. P. Steele, E. J. Sundstrom, H. L. Woodcock, P. M. Zimmerman, D. Zuev, B. Albrecht, E. Alguire, B. Austin, G. J. O. Beran, Y. A. Bernard, E. Berquist, K. Brandhorst, K. B. Bravaya, S. T. Brown, D. Casanova, C.-M. Chang, Y. Chen, S. H. Chien, K. D. Closser, D. L. Crittenden, M. Diedenhofen, R. A. DiStasio, H. Do, A. D. Dutoi, R. G. Edgar, S. Fatehi,

L. Fusti-Molnar, A. Ghysels, A. Golubeva-Zadorozhnaya, J. Gomes, M. W. Hanson-Heine, P. H. Harbach, A. W. Hauser, E. G. Hohenstein, Z. C. Holden, T.-C. Jagau, H. Ji, B. Kaduk, K. Khistyaev, J. Kim, J. Kim, R. A. King, P. Klunzinger, D. Kosenkov, T. Kowalczyk, C. M. Krauter, K. U. Lao, A. Laurent, K. V. Lawler, S. V. Levchenko, C. Y. Lin, F. Liu, E. Livshits, R. C. Lochan, A. Luenser, P. Manohar, S. F. Manzer, S.-P. Mao, N. Mardirossian, A. V. Marenich, S. A. Maurer, N. J. Mayhall, E. Neuscamman, C. M. Oana, R. Olivares-Amaya, D. P. O'Neill, J. A. Parkhill, T. M. Perrine, R. Peverati, A. Prociuk, D. R. Rehn, E. Rosta, N. J. Russ, S. M. Sharada, S. Sharma, D. W. Small, A. Sodt, T. Stein, D. Stück, Y.-C. Su, A. J. Thom, T. Tsuchimochi, V. Vanovschi, L. Vogt, O. Vydrov, T. Wang, M. A. Watson, J. Wenzel, A. White, C. F. Williams, J. Yang, S. Yeganeh, S. R. Yost, Z.-Q. You, I. Y. Zhang, X. Zhang, Y. Zhao, B. R. Brooks, G. K. Chan, D. M. Chipman, C. J. Cramer, W. A. Goddard, M. S. Gordon, W. J. Hehre, A. Klamt, H. F. Schaefer, M. W. Schmidt, C. D. Sherrill, D. G. Truhlar, A. Warshel, X. Xu, A. Aspuru-Guzik, R. Baer, A. T. Bell, N. A. Besley, J.-D. Chai, A. Dreuw, B. D. Dunietz, T. R. Furlani, S. R. Gwaltney, C.-P. Hsu, Y. Jung, J. Kong, D. S. Lambrecht, W. Liang, C. Ochsenfeld, V. A. Rassolov, L. V. Slipchenko, J. E. Subotnik, T. Van Voorhis, J. M. Herbert, A. I. Krylov, P. M. Gill, and M. Head-Gordon, Molecular Physics (2014).

[60] R. Seeger and J. A. Pople, J. Chem. Phys. **66**, 3045 (1977).

[61] P. Pulay, Chem. Phys. Lett. **73**, 393 (1980).

[62] P. Pulay, J. Comp. Chem. **3**, 556 (1982).

[63] A. T. B. Gilbert, N. A. Besley, and P. M. W. Gill, J. Phys. Chem. A **112**, 13164 (2008).

[64] A. J. W. Thom and M. Head-Gordon, Phys. Rev. Lett. **101**, 193001 (2008).

LIST OF FIGURES

1 CO_2 symmetric dissociation, cc-pVDZ basis. 'NC' = noncollinear. Energies are relative to UHF energies of C and (two) O. Compare Fig. 6 of ref. 23. The blue circle on sol. 2 demarcates the unstable and stable regions, the angles above the circle point to the unstable region, and the presence of two angles means that the solution is both GHF → GHF and GHF → cGHF unstable there. Sol. 1 remains stable until around 1.8 Å. 22

2 CO_2 symmetric dissociation, cc-pVDZ basis: collinearity test data for sol. 2. Essentially, this solution is a noncollinear rotation between $m_s = 0$ and $m_s = 1$ UHF states. 23

3 CO_2 symmetric dissociation, cc-pVDZ basis: eigenvalues of A matrix for sol. 1. 24

4 CO_2 symmetric dissociation, cc-pVDZ basis. Main plot: axial expectation values for sol. 1. Essentially, this solution is a noncollinear rotation between $m_s = 0$ and $m_s = 3$ UHF states. Inset: sol. 1 energy. Energy is relative to UHF energies of C and (two) O. Although this solution is unstable to the right of 1.79 Å, it reaches the lowest available dissociation limit. 25

5 CO_2 asymmetric dissociation, cc-pVDZ basis. 'NC' = noncollinear. Energies are relative to UHF energies of CO (bond length = 1.16 Å) and O. Compare Fig. 9 of ref. 23. As in Fig. 1, the circles dermarcate unstable and stable regions. A single angle indicates that there is only a cGHF instability at that point, while a double angle indicates that there are both GHF and cGHF instabilities. The angles point to the corresponding unstable regions. 26

6 CO_2 asymmetric dissociation, cc-pVDZ basis: sol. 1. Energies are relative to UHF energies of CO (bond length = 1.16 Å) and O. For this solution, $\epsilon_0 = 0$ throughout. 27

7 CO_2 asymmetric dissociation, cc-pVDZ basis: sol. 2 collinearity test data. Essentially, this solution is a noncollinear rotation between $m_s = 0$ and $m_s = 1$ UHF states. 28

8 CO_2 asymmetric dissociation, cc-pVDZ basis: axial expectation values for sol. 2. The $\langle \mathbf{S}_y \rangle$ curve is visually indistinguishable from the ϵ_0 curve, which is shown in Fig. 7. 29

FIGURES

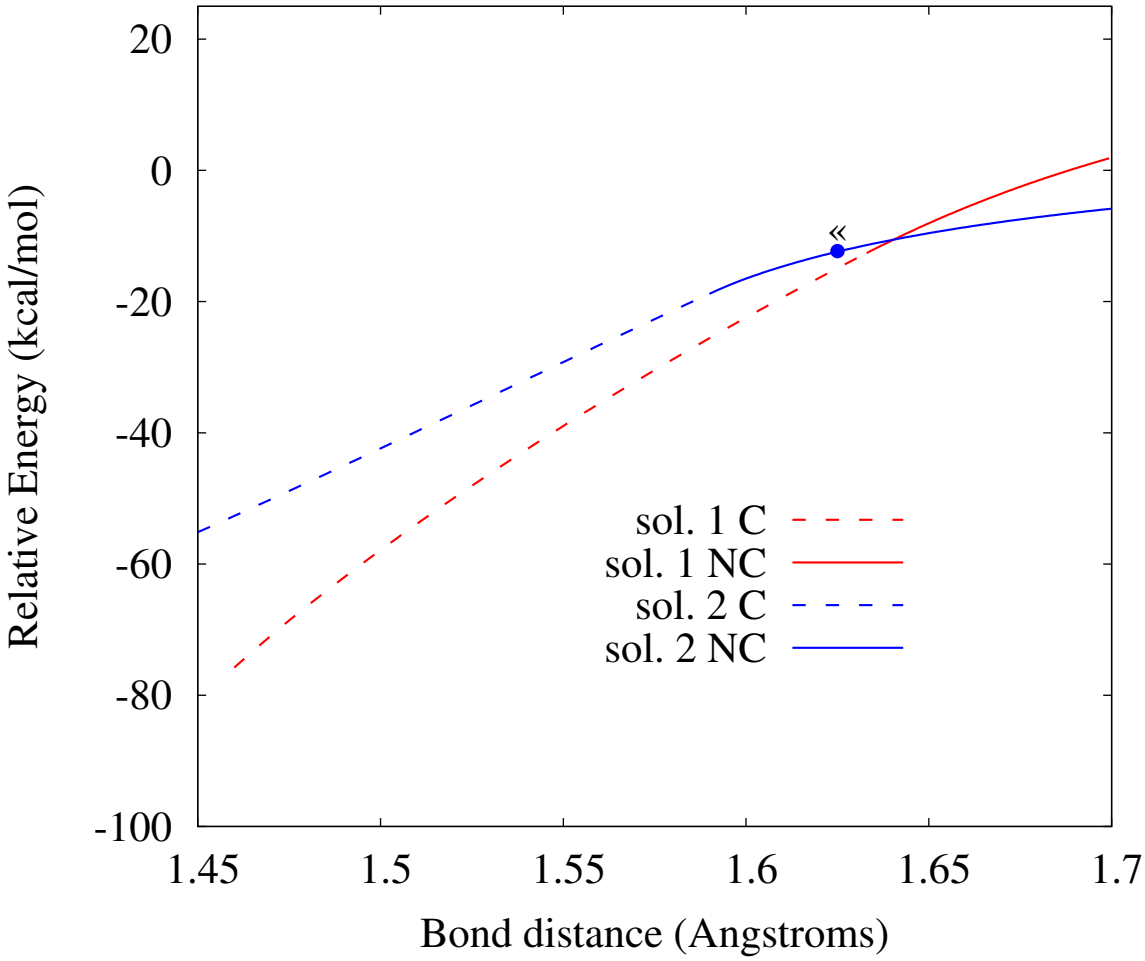

FIG. 1.

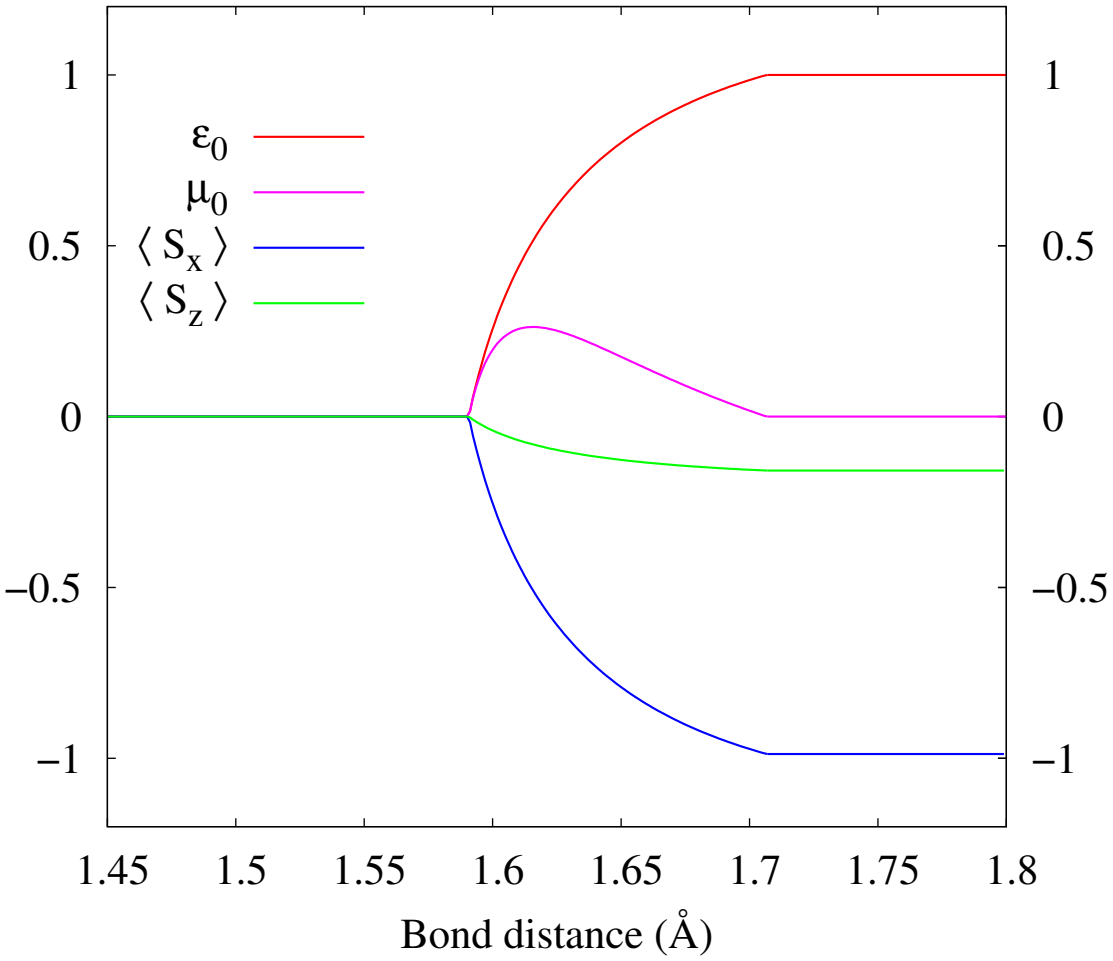

FIG. 2.

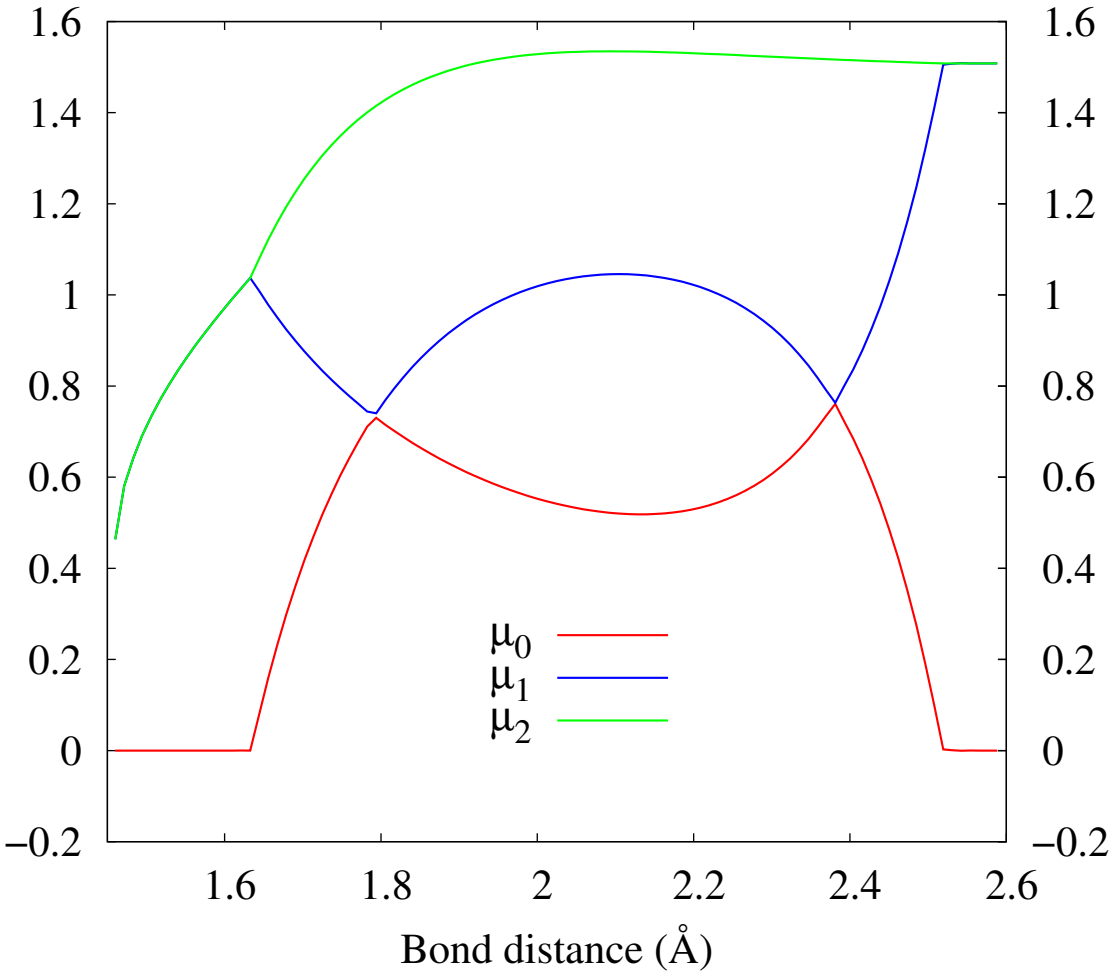

FIG. 3.

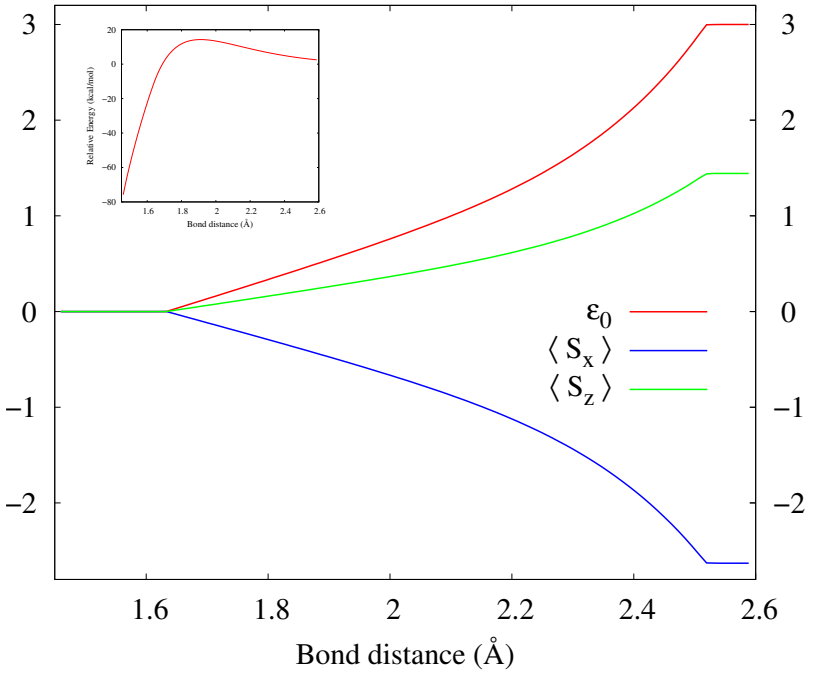
3
2
1
0
−1
−2
1.6
1.8
2
2.2
2.4
2.6
Bond distance (Å)
ε0
⟨ Sx ⟩
⟨ Sz ⟩
Relative Energy (kcal/mol)
20
0
−20
−40
−60
−80

FIG. 4.

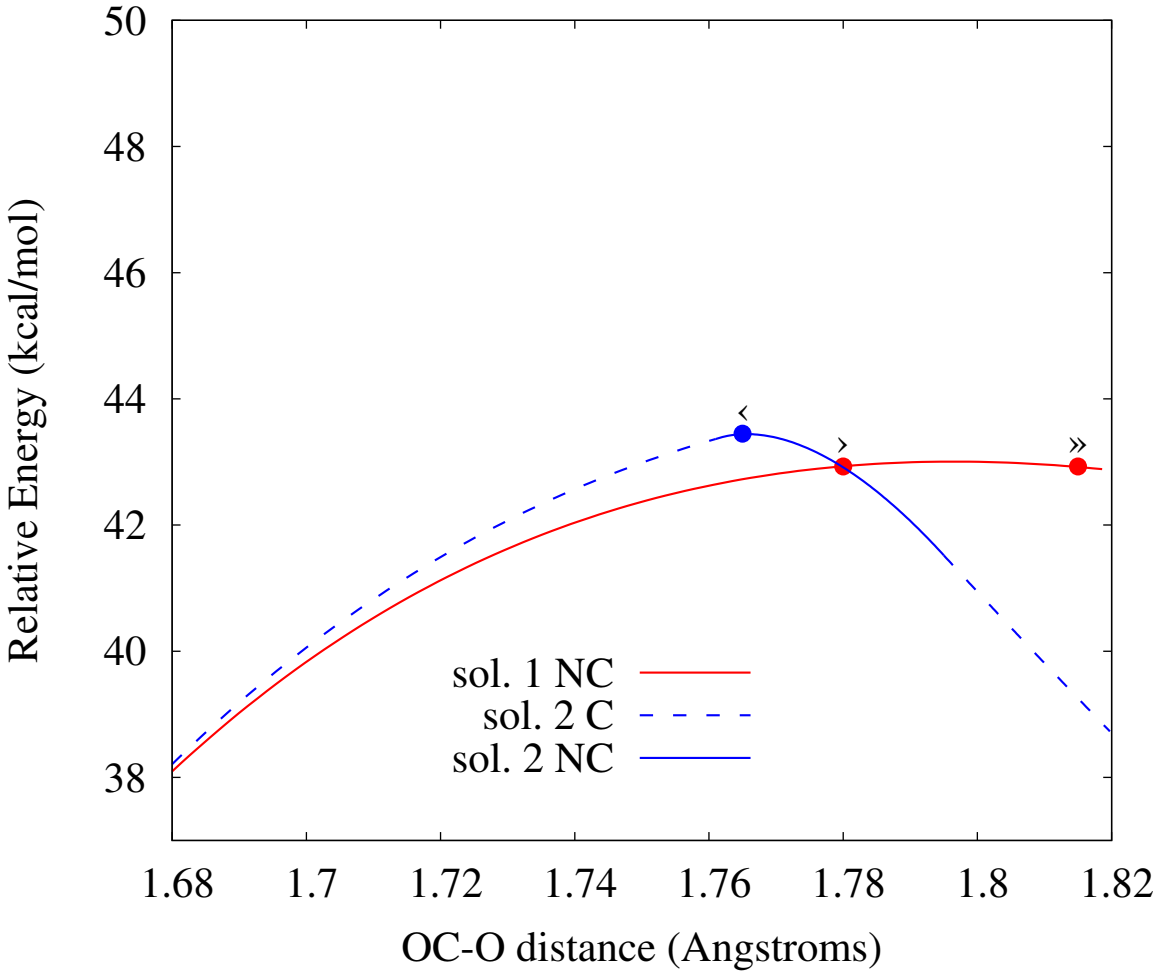
50
48
46
44
42
40
38
Relative Energy (kcal/mol)
1.68
1.7
1.72
1.74
1.76
1.78
1.8
1.82
OC-O distance (Angstroms)
sol. 1 NC
sol. 2 C
sol. 2 NC
‹
›
»

FIG. 5.

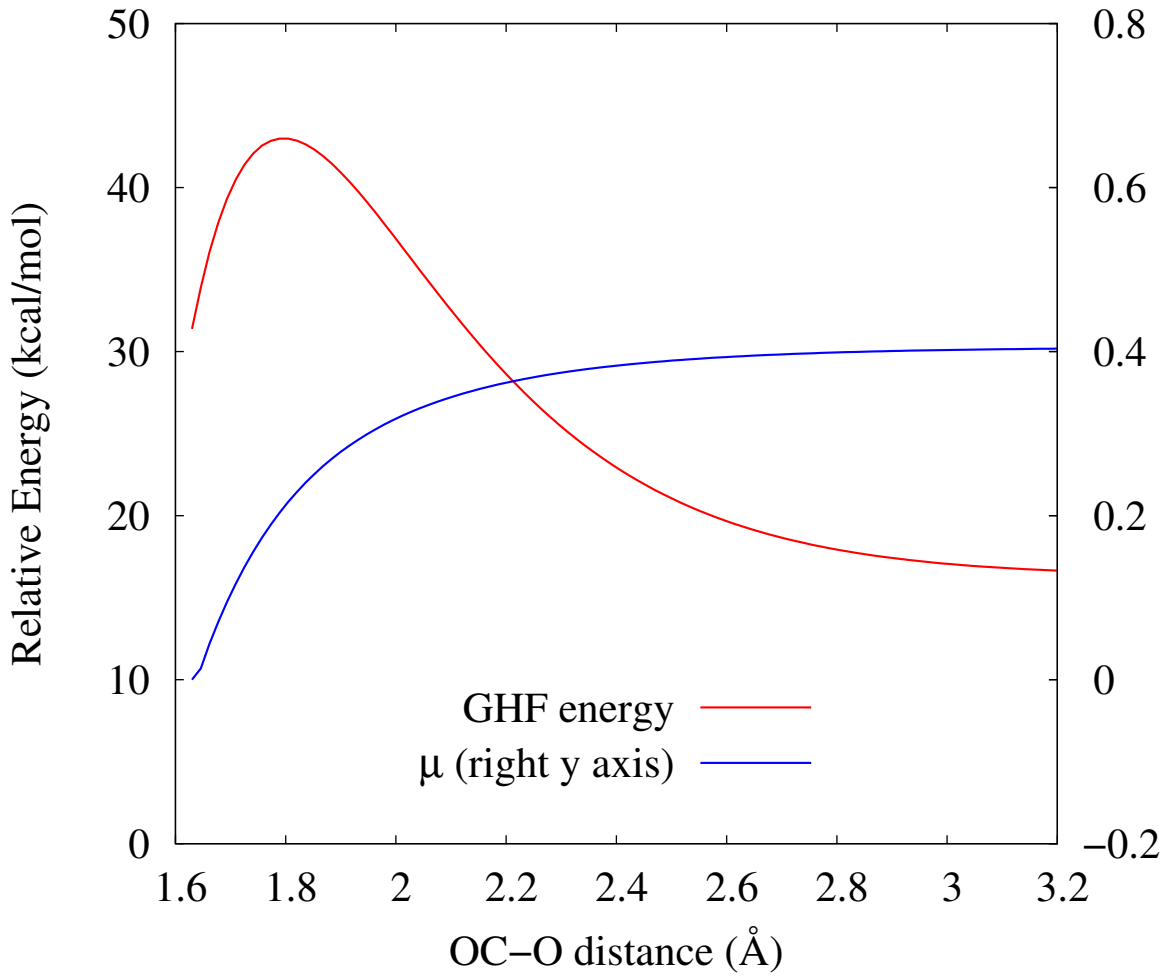
Relative Energy (kcal/mol)
50
40
30
20
10
0
0.8
0.6
0.4
0.2
0
−0.2
1.6
1.8
2
2.2
2.4
2.6
2.8
3
3.2
OC−O distance (Å)
GHF energy
μ (right y axis)

FIG. 6.

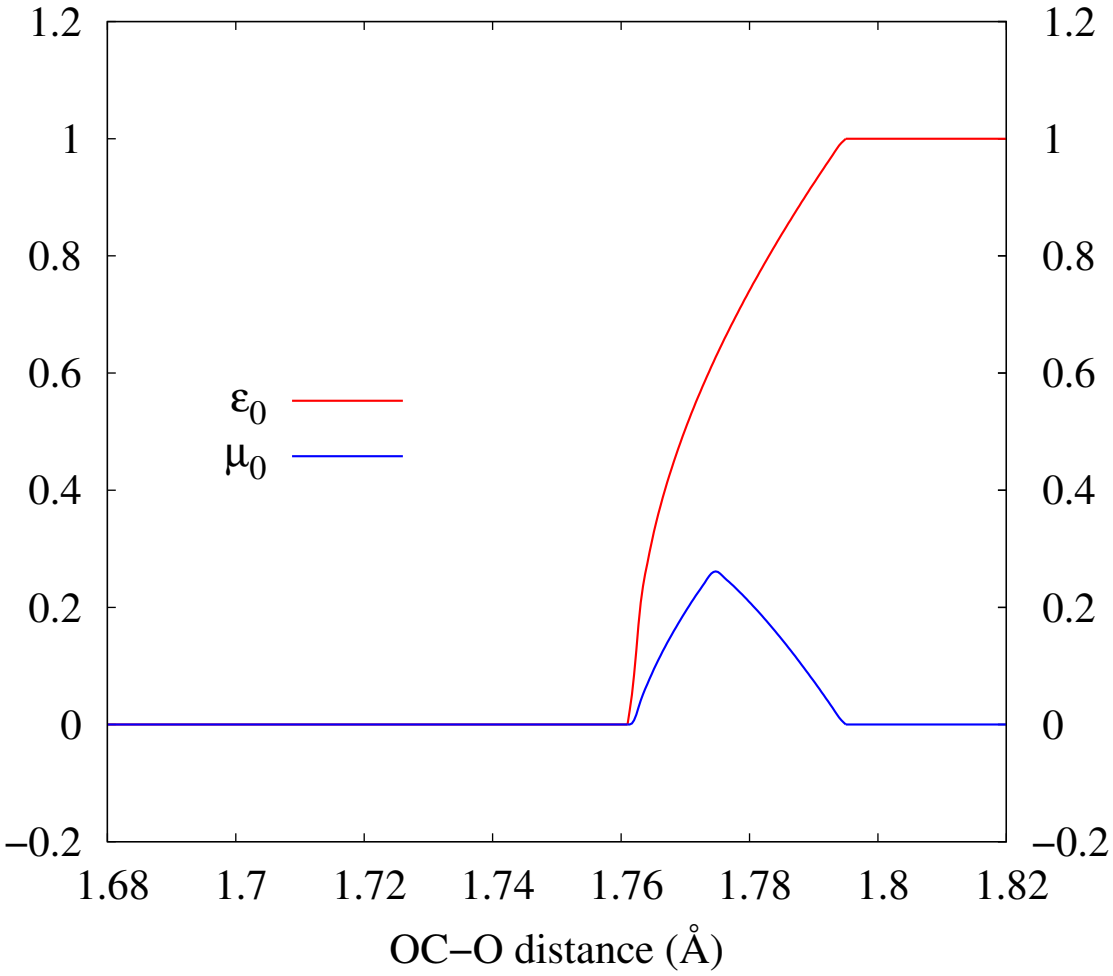
1.2
1
0.8
0.6
0.4
0.2
0
−0.2
1.68
1.7
1.72
1.74
1.76
1.78
1.8
1.82
ε0
μ0
OC–O distance (Å)

FIG. 7.

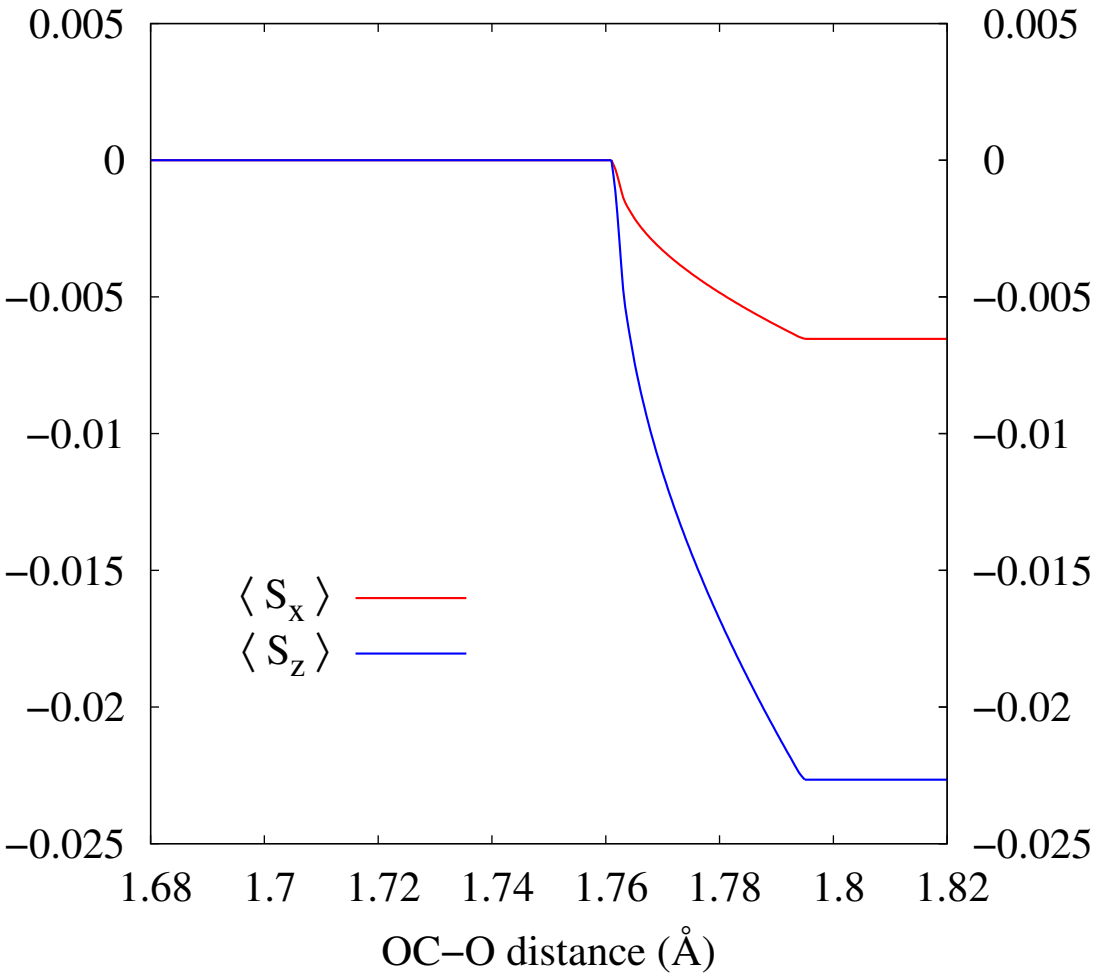
0.005
0
−0.005
−0.01
−0.015
−0.02
−0.025
1.68
1.7
1.72
1.74
1.76
1.78
1.8
1.82
⟨ S_x ⟩
⟨ S_z ⟩
OC−O distance (Å)

FIG. 8.